algorithms

MDPI

Article

Dependent Shrink of Transitions for Calculating Firing Frequencies in Signaling Pathway Petri Net Model

Atsushi Mizuta [1], Qi-Wei Ge [2] and Hiroshi Matsuno [3,*]

[1] Graduate School of Science and Engineering, Yamaguchi University, Yamaguchi 7538512, Japan; v014vc@yamaguchi-u.ac.jp
[2] Faculty of Education, Yamaguchi University, Yamaguchi 7538513, Japan; gqw@yamaguchi-u.ac.jp
[3] Graduate School of Science and Technology for Innovation, Yamaguchi University, Yamaguchi 7538512, Japan
* Correspondence: matsuno@sci.yamaguchi-u.ac.jp; Tel.: +81-83-933-5697

Academic Editors: Henning Fernau and Takeyuki Tamura
Received: 13 August 2016; Accepted: 26 December 2016; Published: 31 December 2016

Abstract: Despite the recent rapid progress in high throughput measurements of biological data, it is still difficult to gather all of the reaction speed data in biological pathways. This paper presents a Petri net-based algorithm that can derive estimated values for non-valid reaction speeds in a signaling pathway from biologically-valid data. In fact, these reaction speeds are reflected based on the delay times in the timed Petri net model of the signaling pathway. We introduce the concept of a "dependency relation" over a transition set of a Petri net and derive the properties of the dependency relation through a structural analysis. Based on the theoretical results, the proposed algorithm can efficiently shrink the transitions with two elementary structures into a single transition repeatedly to reduce the Petri net size in order to eventually discover all transition sets with a dependency relation. Finally, to show the usefulness of our algorithm, we apply our algorithm to the IL-3 Petri net model.

Keywords: signaling pathway; Petri net; retention-free Petri net; dependent shrink; dependency relation

1. Introduction

A Petri net [1,2] is a solid mathematical representation used in concurrent systems modeling, enabling a formal and clear representation of biological pathways at different time and scale levels [3]. Structurally, a Petri net is a directed bipartite graph, including two types of nodes, places and transitions and tokens contained in places. A state of a Petri net is expressed by a token distribution over the places and can be changed by the firing of transitions. The first Petri net model of a biological pathway [4] is a metabolic pathway, describing the conversion of metabolites through enzyme-catalyzed chemical reactions, which has been extensively studied regarding the structural [5–8] and dynamic [9–11] properties.

A signaling pathway is another major biological pathway, consisting of cascades of activated/deactivated proteins or protein complexes, through which signals are propagated from the cell surface to the nucleus. A Petri net has been used as a structural modeling framework for a signal pathway in a knowledge representation [12] and for data implementation in a database [13].

Modularization of a Petri net model into biologically-functional parts in a signaling pathway has been demonstrated using the fundamental behavioral property, T-invariant [14], which was formalized in metabolic pathways before [5–8], and its extended property, the feasible T-invariant [15]. Here, a T-invariant is a firing counting vector of transitions in a periodic firing sequence that leads back to the original token distribution where it starts from. A technique to automatically classify T-invariants into functional modules in a biological pathway was proposed in [16] based on cluster analysis. Another

classification of T-invariants in terms of biological network structure was demonstrated in [17], where hierarchically-structured Petri net representations are derived automatically. T-invariant was further applied for the representation of the enzymatic activation process in a signaling pathway [18]. The dynamic behaviors of a signaling pathway were examined in Petri net models for a token amount, reflecting the concentration levels of molecules obtained based on the order of the transition firings specified by the topological motifs in a signaling pathway [19,20], and were calculated after reducing the number of parameters through a simplification process of a Petri net model [21].

The experimentally uncovered biological facts are usually summarized in a picture of a network structured by figures of various shapes and several type of arrows reflecting biological images. A Petri net allows us to model a biological pathway with maintaining its structural information, owing to the characteristics of the graphical representation of Petri net. Accordingly, Petri net-based modeling does not produce a negative effect of the abstraction in a modeling process compared to other modeling methods, such as differential equation-based methods.

The timed Petri net is a type of Petri net, in which time delay is associated with state transition, and is a promising candidate for modeling the dynamic property of a signaling pathway because the delay time of a transition is able to reflect the rate of a corresponding reaction in a signaling pathway. However, in the works above [18–21], a timed Petri net has not been employed.

The first attempt to use a timed Petri net for the modeling of a signaling pathway was in [22] (the "time" Petri net, which has a different extension in terms of time to the "timed" Petri net, was applied to model metabolic pathways in [11]), where the delay times were calculated based on a simple rule in which the sum of the consumption is equal to the production, so as to maintain the concentration equilibrium for each substance in a signaling pathway. Such Petri nets satisfying this simple rule are called retention-free Petri nets later and introduced as a new concept enabling a more flexible determination of the delay times using a concrete algorithm [23]. Cycles and inhibitory arcs, which often appear in signaling pathways, are treated in [24], but have not been incorporated owing to the difficulties in their structural handling.

These works [22–24] have studied a Petri net-based methodology to calculate estimated values for non-valid reaction speeds from a valid reaction speed, namely a biologically-measured speed, in the signaling pathway. A simple question therefore arises. How many and which reactions should be biologically measured in order to obtain all of the delay times in a Petri net model through the proposed methodology? This paper answers this question by introducing the concept of a "dependency relation" over a transition set of a Petri net, by which the transition set is divided into equivalence classes in the sense of a dependency relation, namely an equivalence relation. In fact, the number of equivalence classes is the number of reactions that should be biologically measured.

One possible way to find such an equivalence class is to establish a series of linear equations for all places based on the retention-freeness, solve the simultaneous equations to obtain the dependent solutions and, finally, determine the transitions with a dependency relation. However, this will take plenty of computation time for a given large-scale signaling pathway model. To cope with this problem, this paper gives an efficient algorithm to reduce the size of a Petri net through a structural analysis and, finally, to discover these equivalence classes.

The remainder of this paper is organized as follows. Section 2 provides the necessary definitions of Petri nets, and Section 3 introduces a timed Petri net and retention-free Petri net ($RFPN$). In Section 4, the concept of a dependency relation over the transitions of $RFPN$ is introduced, and related properties are derived through a structural analysis. In Section 5, based on the theoretical results of Section 4, an algorithm is proposed and applied to the IL-3 Petri net model to show its usefulness. Finally, Section 6 provides some concluding remarks and describes some future works.

2. Basic Definitions and Modeling Rules

In this section, we briefly provide the necessary definitions of a Petri net. For detailed descriptions, the reader is suggested to refer to [2].

Definition 1. *A Petri net (or a net for short), denoted by $PN = (T, P, E, \alpha, \beta)$, is a bipartite graph consisting of elements shown in Figure 1, where:*

- *T is a set of transitions $\{t_1, t_2, \cdots, t_{|T|}\}$;*
- *P is a set of places $\{p_1, p_2, \cdots, p_{|P|}\}$;*
- *$E = E^+ \cup E^-$, and E^+ and E^- are respectively the sets of arcs from transitions to places $e = (t, p)$ and from places to transitions $e = (p, t)$;*
- *α_e is the weight of the arc expressed by positive integer $e = (p, t)$; and*
- *β_e is the weight of the arc expressed by positive integer $e = (t, p)$.*

Figure 1. Petri net elements.

Definition 2. *Let $PN = (T, P, E, \alpha, \beta)$ be a Petri net.*

1. *${}^\bullet t$ ($t^\bullet$) is the set of input (output) places of $t \in T$, and ${}^\bullet p$ ($p^\bullet$) is the set of input (output) transitions of $p \in P$.*
2. *A transition without an input arc is called the source transition, and the set of source transitions is denoted by $T_{src} = \{t_1^{src}, \cdots, t_a^{src}\} (a \geq 1)$.*
3. *A transition without an output arc is called the sink transition, and the set of sink transitions is denoted by $T_{sink} = \{t_1^{sink}, \cdots, t_b^{sink}\} (b \geq 1)$.*
4. *A transition t is called the synchronous transition if there exists a set of input places P_s that for any $p \in P_s$, $p^\bullet = \{t\}$ holds, and is defined by $T_{sync} = \{t_1^{sync}, \cdots, t_c^{sync}\} (c \geq 1)$.*
5. *A place can hold a positive integer that represents a number of tokens. An assignment of tokens in places expressed in the form of a vector M is called a marking, which varies during the execution of a Petri net. Given an initial marking M_0, a Petri net is called a marked Petri net and is denoted by $MPN = (PN, M_o)$.*

Figure 2 shows the source (i) and sink (ii) transitions, and Figure 3 shows a synchronous transition. Note that we use discrete Petri nets in the present study.

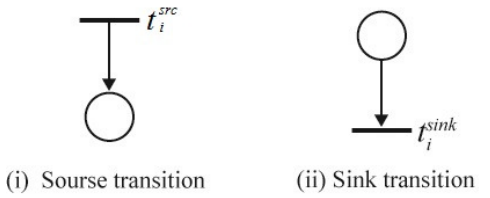

Figure 2. Source and sink transitions.

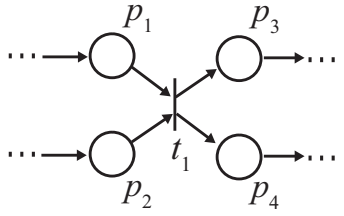

Figure 3. Synchronous transition.

Definition 3. *A transition t is fireable if each input place p_I of PN has at least α_e tokens, where α_e denotes the weight of an arc $e = (p_I, t)$. The firing of a transition t removes α_e tokens from each input place p_I of t and deposits $\beta_e(e = (t, p_O))$ tokens to each output place p_O of t, where β_e denotes the weight of an arc $e = (t, p_O)$. A source transition is always fireable.*

Li et al. [18] gave the following modeling rules for signaling pathways based on a Petri net representation.

1. Places denote static elements, including chemical compounds, conditions, states, substances and cellular organelles participating in the biological pathways. Tokens indicate the presence of such elements. The number of tokens can be regarded as a representation of the amount of chemical substances. The current assignment of tokens to the different places is expressed in the form of a vector, namely a marking, as defined above.
2. Transitions denote active elements, including chemical reactions, events, actions, conversions and catalyzed reactions. A transition fires by taking off tokens from their individual input places and creating new tokens that are distributed to the output places if the input places have at least as many tokens in them as the arc weight from the place to the transition.
3. Directed arcs connecting places and transitions represent the relations between corresponding static elements and active elements. Arc weights α and β (defined in Definition 1) describe the quantities of substances required before and after a reaction, respectively. Particularly in the case of modeling a chemical reaction, arc weights represent quantities given by stoichiometric equations of the reaction itself. Note that the weight of an arc is omitted if the weight is one.
4. Because an enzyme itself acts as a catalyzer in biological pathways, and no consumption occurs in the biochemical reactions, an enzyme is exceptionally modeled in the following definition.
5. An inhibition function in biological pathways is modeled by an inhibitor arc.

Definition 4. *An enzyme in a biological pathway is modeled by a place, called an enzyme place, as shown in Figure 4* [18].

1. *Enzyme place p_i has a self-loop with the same weight connected from and to transition t_s. Once an enzyme place is occupied by a token, the token will return to the place again to maintain the fireable state if the transition t_s is fired.*
2. *Let t_p and t_d denote a token provider of p_i and a sink output transition of p_i, respectively, where the firing of t_p represents an enzyme activation reaction, and the firing of t_d implies a small natural degradation in a biological pathway. p_i holds up token(s) after firing transition t_p, and the weights of the arcs satisfy $\alpha(p_i, t_d) \ll \alpha(p_i, t_s)$.*

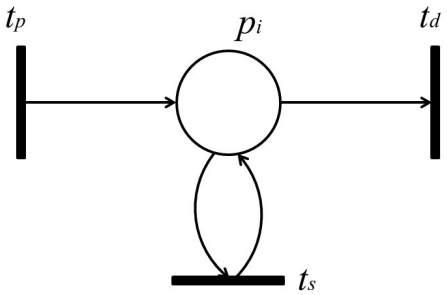

Figure 4. An enzyme place in a Petri net model.

3. Timed Petri Net and Retention-Free Petri Net

Petri nets are extended by assigning a delay time of the firing to each transition to facilitate a system-level understanding through means of a simulation. Such an extended Petri net is called a timed Petri net.

Definition 5. *Timed Petri net TPNis defined by $TPN = (PN, D)$, where D is a set of positive numbers expressing the firing delay times (or delay time for short) of transitions in T. The firing rule of a TPN is as follows:*

1. *initially, all of the tokens are in a non-reserved state; once a transition t_i is decided to have fired, the tokens required for firing are changed from the non-reserved state to the reserved state;*
2. *when the delay time d_i of t_i has passed, t_i fires to remove the reserved tokens from the input places of t_i and put non-reserved tokens into the output places of t_i.*

In a timed Petri net, the firing times of a transition t_i per unit of time are called firing frequency f_i. $\overline{f_i}$ represents the maximum firing frequency of t_i. The delay time d_i of t_i is given by the reciprocal of $\overline{f_i}$.

Note that firing frequencies indicate reaction speed data in a biological pathway.

We show here the method of conflict resolution using stochastic decision rules. To resolve the conflict firing problem, there are three methods that can be adopted: priority, probabilistic choice and alternate firing [25]. The proposed firing rule given in this paper is to combine a probabilistic choice and alternate firing. We introduce a stochastic approach to determine the firings for a series of transitions in conflict (Figure 5), as defined in the following definition.

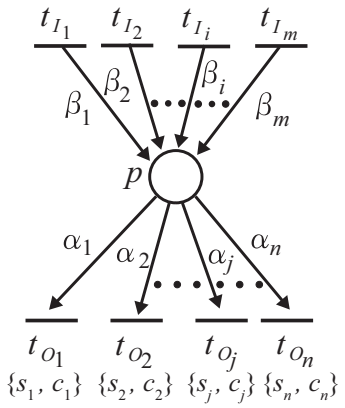

Figure 5. An example illustrating a conflict state.

Definition 6. *Suppose a place p possesses output transitions, $t_{O_1}, t_{O_2}, \cdots, t_{O_n}$, as shown in Figure 5. Then, the firing rule is as follows* [23]*:*

1. *Each unreserved token deposited to input place p is assigned to be reserved by the transition t_{O_j} that satisfies the following expression:*

$$j = \arg\min_{1 \le i \le n} \delta(i), \tag{1}$$

where $\delta(i)$ is decided by the following condition:

$$\delta(i) = \left| \frac{(\lfloor \frac{c_i}{\alpha_i} \rfloor)}{\sum_{k=1}^{n} (\lfloor \frac{c_k}{\alpha_k} \rfloor)} - s_i \right|; \tag{2}$$

2. *When the number of reserved tokens of t_{O_j} is not less than the required token number for the firing, the firing of t_{O_j} is decided;*
3. *After the delay time d_{O_j} of t_{O_j} has passed, t_{O_j} fires to remove the reserved tokens from the input place of t_{O_j} and deposits unreserved tokens into the output places of t_{O_j}.*

In the above expression (2), α_j is the arc weight of $e(p, t_{O_j})$; s_j is the firing probability of transition t_{O_j}, which represents the proportion of the firing frequency of each transition within the total firing frequency of the transitions in conflict. Probability s_j is assigned to the corresponding transition t_{O_j}, which is given as a constant in advance according to the event. Variable c_j is an accumulated number of tokens that t_{O_j} has reserved so far, and thus, $\lfloor \frac{c_j}{\alpha_j} \rfloor$ represents the number of firing times of transition t_{O_j} from the beginning. Expression (2) is designed to reserve the token to such a transition t_i that has the largest difference between the calculated firing probability $\lfloor \frac{c_j}{\alpha_j} \rfloor / \sum_{k=1}^{n} \lfloor \frac{c_k}{\alpha_k} \rfloor$ and the given firing probability s_j among all transitions in conflict.

Definition 7. [23] *With the firing of transition t_I, token amounts flowing into place p per unit of time are called "input token-flow" and are denoted by $TF_{t_I,p}$. On the other hand, with the firing of transition t_O, token amounts flowing out of place p per unit of time are called "output token-flow" and are denoted by TF_{p,t_O}. $TF_{t_I,p}$ and TF_{p,t_O} (shown in Figure 6) are defined by the following equations, respectively:*

$$TF_{t_I,p} = f_I \beta_I \quad (3)$$

$$TF_{p,t_O} = f_O \alpha_O, \quad (4)$$

where f_I and f_O are the firing frequencies of t_I and t_O, respectively, and β_I and α_O are the weights of $e = (t_I, p)$ and $e = (p, t_O)$, respectively.

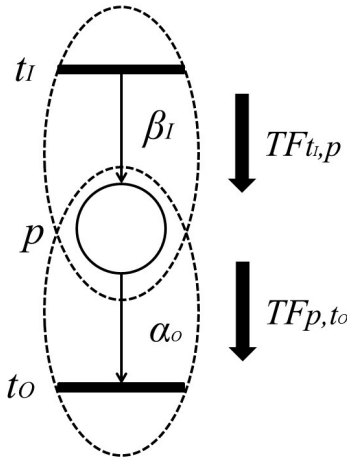

Figure 6. Input and output token flows.

Based on this definition, the following proposition holds.

Proposition 1. [23] *Let p be a place with input transitions $\{t_{I_i} | t_{I_i} \in {}^\bullet p\}$ and output transitions $\{t_{O_j} | t_{O_j} \in p^\bullet\}$. Then, $\sum_{i=1}^{m} TF_{t_{I_i},p}$ and $\sum_{j=1}^{n} TF_{p,t_{O_j}}$ are the total input token-flow and the total output token-flow for place p, respectively. Furthermore, when firing frequency f is at the maximum firing rate, $\overline{f}$, input token-flow $TF_{t_I,p}$ and output token flow TF_{p,t_O} become the maximum, $\overline{FT_{t_I,p}}$ and $\overline{FT_{p,t_O}}$, respectively. These maximum token-flows satisfy the following equations.*

$$\sum_{i=1}^{m} TF_{t_{I_i},p} \leq \sum_{i=1}^{m} \overline{FT_{t_{I_i},p}} \quad (5)$$

$$\sum_{j=1}^{n} TF_{p,t_{O_j}} \leq \sum_{j=1}^{n} \overline{FT_{p,t_{O_j}}} \quad (6)$$

The following requirement is trivial.

Proposition 2. [23] *In a timed Petri net, the total output token-flow is not more than the total input token-flow for each place p:*

$$\sum_{i=1}^{m} TF_{t_{I_i},p} \geq \sum_{j=1}^{n} TF_{p,t_{O_j}}, \tag{7}$$

In a signaling pathway, a reaction not only modifies the formation of molecules, as mentioned above, but also controls the amounts of produced substances. Although the amount of a substance will change along the signal propagation, it cannot be increased indefinitely; otherwise, an abnormal accumulation of a substance may cause a crucial problem in the signaling pathway. Based on this observation, we introduced the notion of a "retention-free" pathway for a timed Petri net. In a retention-free Petri net, the total token amounts flowed-in and flowed-out for each place per unit of time are equivalent.

Definition 8. [23] *A timed Petri net TPN is called a retention-free Petri net (RFPN) (satisfying Proposition 1) if the total input token-flow and total output token-flow are equivalent at any place of TPN, that is,*

$$\sum_{i=1}^{m} TF_{t_{I_i},p} = \sum_{j=1}^{n} TF_{p,t_{O_j}}. \tag{8}$$

In fact, there exists at least one T-invariant in an *RFPN*, which indicates a firing counting vector of transitions in a periodic firing sequence [26] that leads back to the marking where it starts. This is because actually, the firing frequencies of all of the transitions construct a T-invariant.

4. Dependency Relation and Dependent Shrink

The firing frequency of a certain transition can be calculated if the firing frequencies of the transitions attached to that transition have been determined thus far, i.e., when these transitions are dependent on each other with respect to the firing frequencies. To provide a clear and precise definition of this dependency of the transitions, we introduce a new concept called a "dependency relation" for transitions, which is formalized based on the retention-free concept presented in the previous section. After that, we propose a method for shrinking a Petri net subnet, induced by the transitions satisfying a dependency relation, into a single transition. In other words, if a subnet can be shrunk, then the firing frequency of any transition in the subnet can be deduced based on the firing frequency of a certain transition inside the subnet.

4.1. Dependency Relation

Definition 9. *Let TPN be a timed Petri net and t_i and t_j be two transitions. Here, t_i and t_j are said to be related to each other if and only if the following equation holds:*

$$f_i = r_{ij} f_j, \tag{9}$$

where f_i and f_j are the firing frequencies of t_i and t_j, and r_{ij} is a positive rational. This is called a dependency relation and is denoted by $(t_i, t_j) \in R$.

The above equation means if two transitions are related to each other, then firing frequencies are dependent. Based on this definition, we have the following propositions.

Theorem 1. *A dependency relation is an equivalence relation.*

Proof. We only need to prove that a dependency relation is reflexive, symmetric and transitive. Let t, t_1, t_2 and t_3 be transitions of a Petri net. A dependency relation is clearly reflexive and symmetric

because (1) $f_t = f_t$ holds and (2) if $f_1 = r_{12} f_2$, then $f_2 = \frac{1}{r_{12}} f_1$, and vice versa. Suppose $f_1 = r_{12} f_2$ and $f_2 = r_{23} f_3$ hold, then $f_1 = r_{12} r_{23} f_3$, which means the dependency relation is transitive. □

Based on the Definition 9, we have the following proposition for a retention-free Petri net.

Proposition 3. *Let PN_{siso} and PN_{conf} be two retention-free nets consisting of a place with single input and single output transitions (called a single-input and single-output structure), and a conflict place with multiple transitions (called a conflict structure), respectively. (i) In PN_{siso}, the input transition and output transition satisfy a dependency relation; (ii) in PN_{conf}, all output transitions satisfy their dependency relation with one another.*

Proof. (i) Suppose PN_{siso} is a net, as shown in Figure 7. Because Figure 7 is retention free, the amount of input and output token flows through place p must be equal, i.e., $f_i \beta_i = f_o \alpha_o$. Thus, the firing frequency f_i can be expressed as $f_i = \frac{\alpha_o}{\beta_i} f_o$. (ii) Without a loss of generality, herein we suppose place p possesses a single input transition (because we only need to consider the dependency relation of the output transitions), as shown in Figure 8.

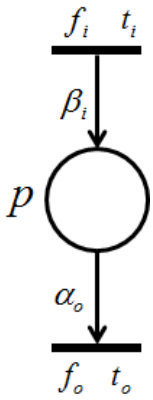

Figure 7. Single-input and single-output structure (PN_{siso}).

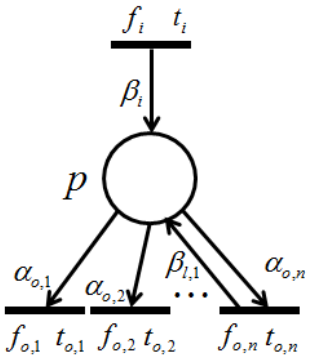

Figure 8. Conflict structure (PN_{conf}).

Since the given firing probabilities of all output transitions, $s_{o,1}, s_{o,2}, \cdots, s_{o,n}$, satisfy:

$$\begin{array}{rcl} \frac{s_{o,1}}{s_{o,2}} & = & \frac{f_{o,1}}{f_{o,2}} \\ \frac{s_{o,1}}{s_{o,3}} & = & \frac{f_{o,1}}{f_{o,3}} \\ & \vdots & \\ \frac{s_{o,1}}{s_{o,n}} & = & \frac{f_{o,1}}{f_{o,n}}. \end{array} \tag{10}$$

the firing frequencies, $f_{o,2}, f_{o,3}, \cdots, f_{o,n}$, can be expressed through the following equations:

$$\begin{array}{rcl} f_{o,2} & = & \frac{s_{o,2}}{s_{o,1}} f_{o,1} \\ f_{o,3} & = & \frac{s_{o,3}}{s_{o,1}} f_{o,1} \\ & \vdots & \\ f_{o,n} & = & \frac{s_{o,n}}{s_{o,1}} f_{o,1}, \end{array} \tag{11}$$

which means that all output transitions satisfy the dependency relations with one another. □

The two nets shown above are elementary structures of *RFPN*, which will be applied in the following discussion, as well as in our algorithm.

As shown in Theorem 1 above, a dependency relation is an equivalence relation. Hence, the transition set of a timed Petri net can be divided into independent subsets, i.e., equivalence classes. In the following subsection, to indicate a block of a retention-free Petri net, in which all transitions satisfy a dependency relation, we provide a definition of "dependent shrink".

4.2. Dependent Shrink

Definition 10. *Let $PN = (T, P, E, \alpha, \beta)$ be a retention-free Petri net.*

(i) Let T_x be a subset of T, where x ($1 \leq x \leq |T|$) is a positive integer, and all of the transitions in T_x satisfy a dependency relation. A Petri net induced by T_x is defined as $PN_x = (T_x, P_x, E_x, \alpha, \beta)$, where $P_x = \{p | p \in {}^\bullet t \cup t^\bullet, t \in T_x\}$, and $E_x = \{e | e \in T_x \times P_x \cup P_x \times T_x\}$.

(ii) The transformation of PN_x by constructing all transitions of T_x and any place $p \in P_x$ satisfying ${}^\bullet p \cup p^\bullet \subset T_x$ into a single transition, denoted by t_x, is called a dependent shrink. In addition, the resultant net $PN' = (T', P', E', \alpha, \beta)$ transformed from PN is called a dependent shrunk net, where, $T' = T - T_x + t_x$, $P' = P - \{p | {}^\bullet p \cup p^\bullet \subset T_x\}$, $E' = \{e | e \in T' \times P' \cup P' \times T'\}$, α and β of t_x's input and output arcs are decided, such that the input and output token flows of the places, included in ${}^\bullet t_x \cup t_x^\bullet$, are kept equivalent before and after shrinking.

The following lemma shows us that the dependency relation of the transitions does not change before and after a dependent shrink, i.e., if two transitions are out of the dependency relation, then they will not satisfy the dependency relation after a dependent shrink; and vice versa.

Lemma 1. *Let $PN = (T, P, E, \alpha, \beta)$ be a retention-free net including a subnet $PN_x = (T_x, P_x, E_x, \alpha, \beta)$ of Figure 9a or Figure 10a and $PN' = (T', P', E', \alpha, \beta)$ be its dependent shrunk net by applying a dependent shrink for PN_x, where $T' = T - T_x + t_x$. Suppose $t_j, t_k \in T - T_x$ and $t_y \in T_x$; then, the following claims hold.*

Claim 1: If $(t_j, t_k) \in R$ in PN, then $(t_j, t_k) \in R$ in PN'; otherwise, $(t_j, t_k) \notin R$ in PN'.

Claim 2: If $(t_j, t_y) \in R$ ($(t_k, t_y) \in R$) in PN, then $(t_j, t_x) \in R$ ($(t_k, t_x) \in R$) in PN'; otherwise, $(t_j, t_x) \notin R$ ($(t_k, t_x) \notin R$) in PN'.

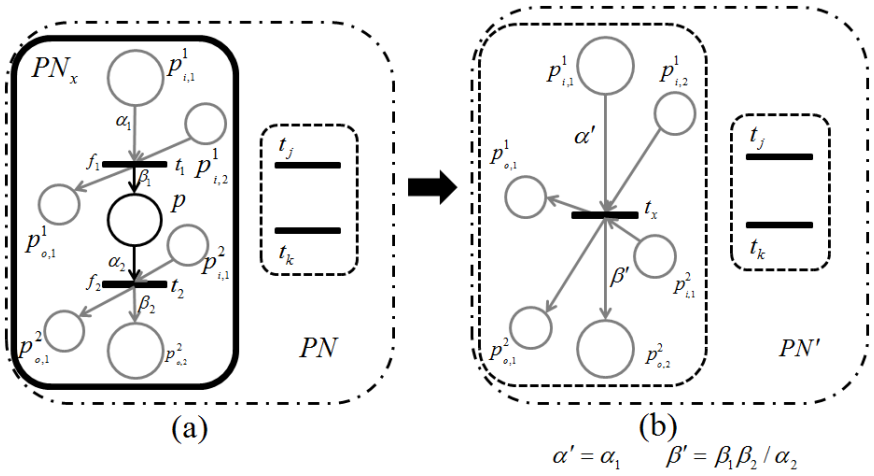

Figure 9. Shrink of a single-input and single-output structure. (**a**) before shrinking; (**b**) after shrinking.

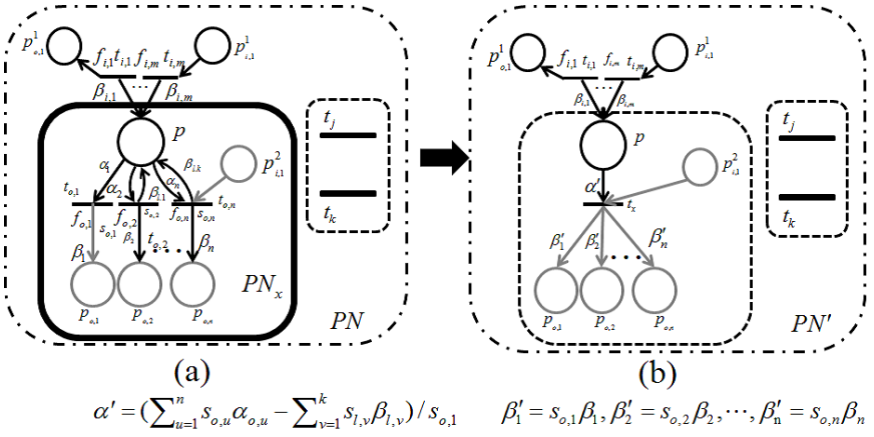

Figure 10. Shrink of a conflict and self-loop structure. (**a**) before shrinking; (**b**) after shrinking.

Proof. Recall that a single-input and single-output structure (Figure 7) and a conflict structure (Figure 8) are the elementary structures of *RFPN* considered in this paper. PN_xs surrounded by the bold line in Figures 9a and 10a are basically the same as in Figures 7 and 8, respectively, but these are extended by attaching additional places and arcs (pale parts) in order to make them more general. In addition, two transitions, t_j and t_k, are appended for the proof of Lemma 1 below.

For the case of Figure 9, p and its input and output transitions (t_1 and t_2) are shrunk into a single transition, t_x, and the weights of the new input and output arcs are given as $\alpha' = \alpha_1$ and $\beta' = \beta_2 \frac{\beta_1}{\alpha_2}$, respectively. On the other hand, for the case of Figure 10, all output transitions of place p are shrunk into a single transition, t_x, and the weights of the new input and output arcs are set to:

$$\begin{aligned} \alpha' &= \left(\sum_{u=1}^{n} s_{o.u}\alpha_{o.u} - \sum_{v=1}^{k} s_{l.v}\beta_{l.v} \right) / s_{o.1} \\ \beta'_1 &= s_{o.1}\beta_1 \\ \beta'_2 &= s_{o.2}\beta_2 \\ &\vdots \\ \beta'_n &= s_{o.n}\beta_n. \end{aligned}$$

Here, $\alpha' > 0$ should be satisfied; otherwise, *PN* is not a retention-free Petri net. For both of these two cases, the moderated tokens on ${}^\bullet t_j \cup t_j^\bullet$ and ${}^\bullet t_k \cup t_k^\bullet$ arising from the firings of t_1 and t_2 of Figure 9a

and the firings of $t_{o,1}, t_{o,2}, \cdots, and\ t_{o,n}$ of Figure 10a have no changes before or after shrinking PN_x; that is, the dependency relation between t_j and t_k is not changed, and Claim 1 therefore holds.

Let us see Claim 2. t_y should be the input or output transition of p in Figure 9 and one of the output transitions of p in Figure 10. Similar to the proof of Claim 1, the moderated tokens on ${}^\bullet t_j \cup t_j^\bullet$ and ${}^\bullet t_k \cup t_k^\bullet$ arising from the firings of t_1 and t_2 of Figure 9a and the firings of $t_{o,1}, t_{o,2}, \cdots, and\ t_{o,n}$ of Figure 10a have no changes before or after shrinking PN_x. Hence, if $(t_j, t_y) \in R$ (or $(t_k, t_y) \in R$) in PN, then $(t_j, t_x) \in R$ (or $(t_k, t_x) \in R$) in PN'; oppositely, if $(t_j, t_x) \in R$ (or $(t_k, t_x) \in R$) in PN', then t_j (or t_k) is related to any transition of Figure 9 or Figure 10. Therefore, this lemma holds. □

The changes of weights given in the proof of Lemma 1 are also applied in our proposed algorithm.

In the following subsection, the uniqueness of a dependent shrink is proven. This means that if a retention-free Petri net Q can be transformed into a dependent shrunk net, the order of transitions in Q for the transformation does not affect the final resultant net.

4.3. Uniqueness on Dependent Shrink

In this section, we introduce the concept of a dependent transition set that is a maximum set of transitions with a dependency relation and discuss the uniqueness of the resultant net through dependent shrink for retention-free Petri nets.

Definition 11. *Let $PN = (T, P, E, \alpha, \beta)$ be a retention-free net, t be a transition in T and T_t be a set of all transitions related to t.*

(i) Such a T_t is called a t-dependent transition set.

(ii) A Petri net induced by T_t is called a t-dependent subnet and is denoted by $PN_t = (T_t, P_t, E_t, \alpha, \beta)$.

Note that, differing from PN_x defined in Definition 10, the transitions included in PN_t are not related to any transitions of $T - T_t$ owing to the fact that T_t is a maximum set of transitions with a dependency relation (shown in Figure 11). The following lemma is immediate.

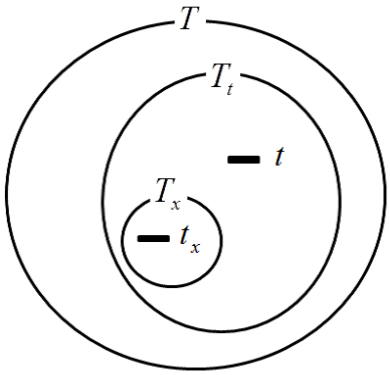

Figure 11. Relationships among T_x, T_t and T.

Lemma 2. *Let T_t and $T_{t'}$ be the transition sets of t-dependent and t′-dependent, respectively. If $(t, t') \in R$, then $T_t = T_{t'}$.*

Lemma 3. *Let T_t be a t-dependent transition set and PN_t be its t-dependent subnet of a retention-free Petri net PN. Then, PN_t is a connected subnet.*

Proof. Assume that PN_t is not connected, i.e., PN_t consists of at least two divided nets, PN_1 and PN_2. Let us see $PN_1 = (T_1, P_1, E_1, \alpha, \beta)$ and its connection to the other part of PN. There exists a subset $P_1' \subset P_1$ of places that includes all places connecting with the outside transitions (not included in T_1), for instance, T_o. Thus, these transitions of T_o are the only ones that connect PN_1 to other parts

of PN, and further, they are not related to any one of T_t ($(t_o, t) \notin R$ for $t_o \in T_o$ and $t \in T_t$); otherwise, $T_o \subset T_t$. Because PN_1 and PN_2 are not connected, any transition of PN_2 connecting to a transition of PN_1 should pass through at least one of T_o, which implies that the transitions of PN_2 are not related to T_1, and thus, this contradicts that T_t is a t-dependent transition set. □

Theorem 2. *Let t be a transition of a retention-free Petri net $PN = (T, P, E, \alpha, \beta)$, T_t be a t-dependent transition set, $PN_t = (T_t, P_t, E_t, \alpha, \beta)$ be a t-dependent subnet, $PN' = (T', P', E', \alpha, \beta)$ be a net by shrinking PN_t and t_t be a shrunken transition of PN_t. For $t_i, t_j \notin T_t$, $(t_i, t_t) \notin R$ and $(t_j, t_t) \notin R$ are satisfied in PN'. Further, if $(t_i, t_j) \in R$ in PN, then $(t_i, t_j) \in R$ in PN', and vice versa.*

Proof. There exists a subset $P'_t \subset P_t$ of places that includes all places connecting with the outside transitions (not included in T_t), for example, T_o. Thus, these transitions of T_o are only those that connect PN_t to other parts of PN, and further, they are not related to any of T_t ($(t_o, t) \notin R$ for $t_o \in T_o$ and $t \in T_t$); otherwise, $T_o \subset T_t$. After shrinking PN_t, P'_t and t_t remain in $PN' = (T', P', E', \alpha, \beta)$, and of course, $(t_o, t_t) \notin R$ holds in PN' for $t_o \in T_o$. Further, any transition t' included in $T' - \{t_t\}$ connecting to t_t should pass through at least one of T_o, which means that $(t_i, t_t) \notin R$ and $(t_j, t_t) \notin R$ hold for $t_i, t_j \notin T_t$. Furthermore, shrinking PN_t does not destroy the dependency relation for any transitions of T_o, as can be seen in Figures 12 and 13 and, thus, for the transitions of $T' - T_o - \{t_t\}$. Therefore, this theorem holds. □

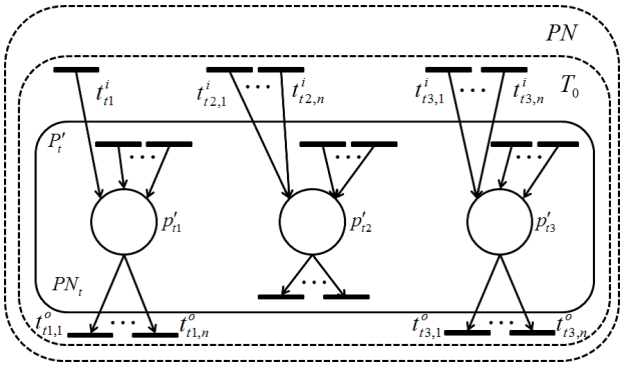

Figure 12. Before shrinking PN_t.

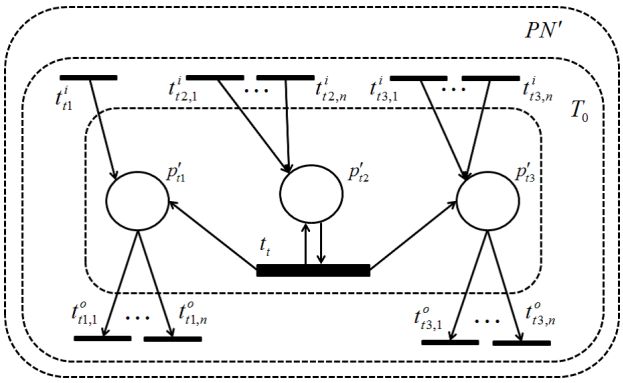

Figure 13. After shrinking PN_t.

According to Theorem 2, if we find all dependent subnets and shrink them individually into single transitions, then all of these transitions are representative of the equivalence classes because a dependency relation is an equivalence relation. The following corollary is immediate.

Corollary 1. *Suppose a retention-free Petri net PN consists of k subnets, $PN_{t_1}, PN_{t_2}, \cdots, PN_{t_k}$, each of which is a dependent subnet. Not depending on the order of dependent shrink for $PN_{t_1}, PN_{t_2}, \cdots, PN_{t_k}$, a unique structure of a resultant net consisting of k transitions can be obtained.*

From Lemma 1 and Theorem 2, we can simply obtain the following result.

Corollary 2. *Iterating a dependent shrink for the cases shown in Figures 9 and 10, a unique resultant net can be obtained.*

5. Dependent Shrink Algorithm and Case Study

In this section, we propose the dependent shrink algorithm based on the discussion in the last section and apply this algorithm to the IL-3 signaling pathway Petri net model (shown in Figure 15), which is transformed from the IL-3 phenomenon model (shown in Figure 14) obtained from the website [27], as a case study. Note that IL-3 is a glycoprotein and is known to be involved in the immune response [28–30].

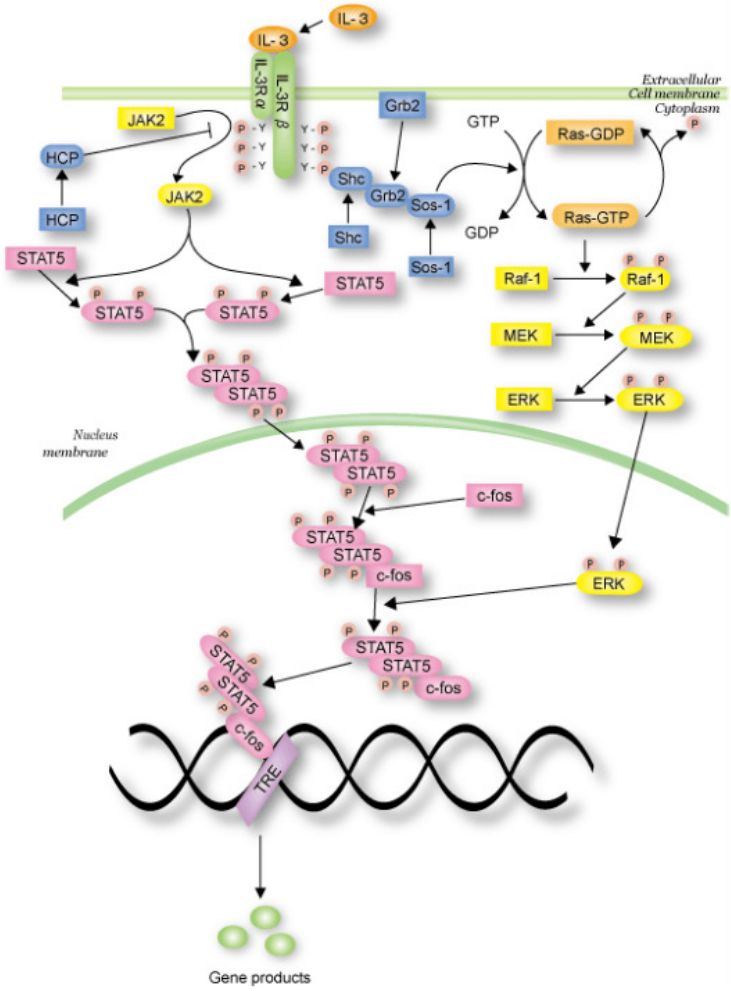

Figure 14. IL-3 signaling pathway [27].

5.1. Outline of Shrink Process

The outline of the dependent shrink process can be briefly described as follows:

Step 1: Shrinking of self-loop structure:
A place randomly selected from a Petri net is stored in a queue after the conversion of the self-loops and the structures of conflict (as shown in Figure 10).

Step 2: Shrink of conflict structure:
If a place picked up from the queue has a self-loop or a transition of one-input and one-output (as shown in Figure 9), this place is shrunk.

Step 3: Changing weight of the input arc:
If a shrunk Petri net has a place with multiple input transitions, then enqueue and continue to Step 2. This procedure is repeated until the queue becomes empty or the number of places with multiple input transitions equals the length of the queue.

The variables used in the algorithm are as follows:

- PN_0 is a given signaling pathway Petri net model constituted by $T_0, P_0, and\ E_0$.
- N is a variable that stores the Petri net after dependent shrink, constituted by T, P and E.
- Q is a queue.
- X is a set of places initially set as a given place set, P_0.
- f is a flag by which a dependent shrink pattern is determined.
- c is a counter, which counts the number of places in Q with multiple input transitions.

5.2. Dependent Shrink Algorithm

The following algorithm is used to repeatedly shrink the structures of Figures 9 and 10 to find transitions with an interdependent firing frequency.

Algorithm 1 Dependent Shrink

Input: $PN_0 = (T_0, P_0, E_0)$
Output: Shrunk Petri net $N = (T, P, E)$
Main(PN_0)
1°$T \leftarrow T_0$, $P \leftarrow P_0$, $E \leftarrow E_0$, $N \leftarrow (T, P, E)$
2°$X \leftarrow P$, $Q \leftarrow \phi$, $c \leftarrow 0$
3°**while** $(X \neq \phi)$
    Pull an element x from $X(X \leftarrow X - \{x\})$
    Enqueue(Q, x)
    Shrink1(N, x)
4°**Shrink2**(N, Q, c)
Shrink1(N, x)
1°**if** $(|{}^\bullet x \cap x^\bullet| \geq 1)$ **then**
        $f \leftarrow 1$
        Arcweight(N, x, f)
2°**if** $(|x^\bullet| \geq 2)$ **then**
    $f \leftarrow 2$
    Arcweight(N, x, f)
Shrink2(N, Q, c)
1°**while** $(|Q| \geq 1)$
    $x \leftarrow$ **Dequeue**(Q)
        if $(|{}^\bullet x \cap x^\bullet| \geq 1)$ **then**
            $f \leftarrow 1$
            Enqueue(Q, x)
            $c \leftarrow 0$

Algorithm 1 *Cont.*

else if ($|^\bullet x| = |x^\bullet| = 1$) **then**
$f \leftarrow 3$
$c \leftarrow 0$
else if ($|^\bullet x| \geq 2$) **then**
$f \leftarrow 4$
Enqueue(Q, x)
$c \leftarrow c + 1$
if ($f \neq 4$) **then**
Arcweight(N, x, f)
if ($c = |Q|$) **then**
Break

Arcweight(N, x, f)
1°**if** ($f = 1$) **then**
$\forall t' \in {}^\bullet x \cap x^\bullet$
$\alpha(x, t') = \alpha(x, t') - \beta(t', x)$
if ($\alpha(x, t') < 0$) **then**
$\beta(t', x) = |\alpha(x, t')|$
$E \leftarrow E - \{(x, t')\}$
else if ($\alpha(x, t') > 0$) **then**
$E \leftarrow E - \{(t', x)\}$
else if ($\alpha(x, t') = 0$) **then**
$E \leftarrow E - \{(t', x), (x, t')\}$
2°**else if** ($f = 2$) **then**
$T \leftarrow T \cup \{t'\}$
$E \leftarrow E \cup \{(x, t')\} \cup \{(u, t') | u \in {}^\bullet z, z \in x^\bullet\} \cup \{(t', v) | v \in z^\bullet, z \in x^\bullet\}$
Choose $z' \in x^\bullet$.
$\forall z \in x^\bullet - \{t'\}$
$\alpha(x, t') = \alpha(x, t') + s(z) * \alpha(x, z)$
$\forall v \in z^\bullet, z \in x^\bullet$
$\beta(t', v) = s(z) * \beta(z, v)$
$\forall u \in {}^\bullet z, z \in x^\bullet$
$\alpha(u, t') = s(z) * \alpha(u, z) / s(z')$
$\alpha(x, t') = \alpha(x, t') / s(z')$
$T \leftarrow T - \{z | z \in x^\bullet - \{t'\}\}$
3°**else if** ($f = 3$) **then**
$T \leftarrow T \cup \{t'\}$
Let z_i, z_o be $\{z_i\} = {}^\bullet x$, $\{z_o\} = x^\bullet$ (due to $|^\bullet x| = |x^\bullet| = 1$).
$E \leftarrow E \cup \{(u, t') | u \in {}^\bullet z_i \cup {}^\bullet z_o\} \cup \{(t', v) | v \in z_i^\bullet \cup z_o^\bullet\}$
$\forall u \in {}^\bullet z_i$
$\alpha(u, t') = \alpha(u, z_i)$
$\forall u \in z_i^\bullet$
$\beta(t', u) = \beta(z_i, u)$
$\forall v \in {}^\bullet z_o$
$\alpha(v, t') = \beta(z_i, x) * \alpha(v, z_o) / \alpha(x, z_o)$
$\forall v \in z_o^\bullet$
$\beta(t', v) = \beta(z_i, x) * \beta(z_o, v) / \alpha(x, z_o)$
$T \leftarrow T - \{z_i | z_i \in {}^\bullet x\} - \{z_o | z_o \in x^\bullet\}$
$P \leftarrow X - \{x\}$

The Algorithm 1 will terminate when all places are shrunk, i.e., a single transition remains, or becomes ones with multiple input transitions and a single output transition. The time complexity is $O(|P||E|)$. As a result, given with a retention-free Petri net, this algorithm gives a smaller shrunk net, in which a transition may represent a class of ones with a dependency relation.

5.3. Case Study

Here, we give an example showing an application of our proposed algorithm. Since the algorithm has not been implemented, here we manually apply it. The algorithm is applied to the IL-3 Petri net model (see Figure 15a), obtained from the website [27]. As a result, the original IL-3 Petri net model shown in Figure 15a is shrunk into Figure 15c. This means that the firing frequencies of all transitions in Figure 15a are dependent on one another. In the intermediate shrunk net (see Figure 15b), by assuming that the firing frequency f_i of the input transition t_i is one, and the weights of the input and output arcs are $\frac{1}{2}$ and one, respectively, then the firing frequency f_o of output transition t_o is $\frac{1}{2}$. In this way, we can calculate all firing frequencies in the IL-3 Petri net model if the firing frequency of one transition is known in this model.

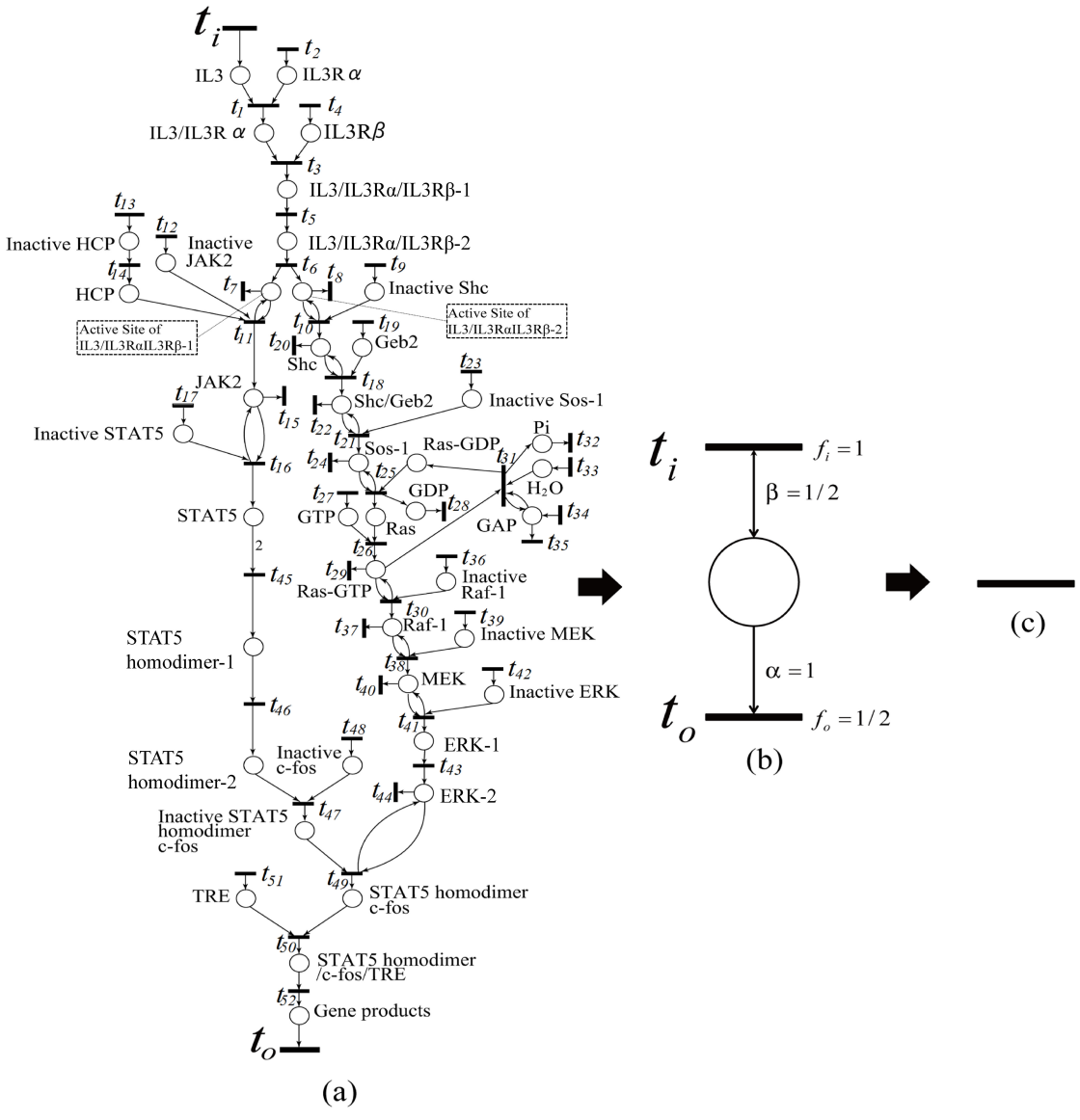

Figure 15. Shrinking processes of the IL-3 Petri net model. (**a**) Petri net model of IL-3; (**b**) intermediate shrunk net; (**c**) final shrunk net.

That is, all of the reaction speed data of the IL-3 Petri net model are dependent on one another, and thus, if one reaction speed datum is available, all of the others can be derived from it.

We have two ways to determine reaction speed data in biological pathway, i.e., firing frequencies. One is to find firing frequency relationships between transitions from the intermediate shrunk nets generated during the execution of the Algorithm 1, in turn from the final net to the original net.

In the intermediate shrunk net (see Figure 15b), by assuming the firing frequency f_i of the input transition t_i to be available (say one), then the firing frequency f_o of output transition t_o is $\frac{1}{2}$. Recursively, we can derive all of the firing frequencies in the IL-3 Petri net model.

Another way is to establish a series of linear equations for all of the places according to retention-freeness, Equation (8), and to solve these equations to finally get the solutions with the form $f_{nonvalid} = r_{nonvalid,valid} f_{valid}$. Here, $f_{nonvalid}, f_{valid}$ are the firing frequencies corresponding to non-valid and valid reaction speed data.

Suppose t_i is only one transition whose corresponding speed data are valid; we can derive the firing frequencies for all of the other transitions of the IL-3 Petri net model in any one of two ways as follows:

$$\begin{aligned} f_i = &\quad f_1 = f_2 = \cdots = f_{28} = 1 \\ f_{29} = &\quad f_{30} = \cdots = f_{50} = f_o = \frac{1}{2}. \end{aligned} \tag{12}$$

In addition to IL-3, we also apply our algorithm to the endocytosis Petri net model and give the shrunk result as can be found in the Supplementary Materials, in which, IL-3 and endocytosis respectively consist of 43 places, 54 transitions and 109 arcs and 24 places, 34 transitions and 70 arcs. Moreover, the System Biology Markup Language (SBML) [31] and Petri Net Markup Language (PNML) [32] files of those Petri net models can also be obtained from the Supplementary Materials.

5.4. Discussion on the Resultant Structure from the Algorithm

As mentioned, when the Algorithm 1 terminates, there are two possible cases: (1) the resultant net is a single transition; (2) the resultant net is such that all places possess a single output transition and multiple input transitions.

Case (1) indicates that all transitions of the given net PN satisfy a dependency relation, and they comprise an equivalence class, that is, if the firing frequency of any one of the transitions is decided, then the frequencies of all of the others are automatically decided as well.

Case (2) may be further divided into: (i) the remaining net consisting of only such transitions that do not satisfy dependency relations with one another; and (ii) some of the transitions satisfying a dependency relation, but not having been shrunk into a single transition.

Case (2) (i) indicates that all transitions in the remaining net are independent, and each is a representative of an equivalence class, as can be illustrated in Figure 16. In this Figure 16a, each transition set is rounded by a line, and the transitions included in each set satisfy a dependency relation with one another. Applying dependent shrink, the transformed net is obtained as shown in Figure 16b. Further, the equivalence classes of PN represented by $t_1, t_2, t_3, t_7, t_8, t_9, t_{10}$ are shown in Figure 16c.

Case (2) (ii) implies that the remaining net includes a subnet that consists of transitions that all have a dependent relation, but cannot be shrunk into a single transition by shrinking the single-input and single-output structure (Figure 7) or the conflict structure (Figure 8). PN'_{t_2}, shown in Figure 17, is such a subnet, where each transition has at least one input place with one output, which means $|P'_{t_2}| \geq |T'_{t_2}|$ in PN'_{t_2}. To find such a subnet, we should establish a series of linear equations for all places according to the retention-freeness in which the input and output token flows are equal and solve these equations. Because $|P'_{t_2}| \geq |T'_{t_2}|$ in PN'_{t_2}, the number of equations is more than that of the variables (firing frequencies of the transitions). Thus, if there are exactly $|T'_{t_2}| - 1$ linear independent equations,

then all of the transitions satisfy a dependency relation. A detailed discussion of this remains as a future issue.

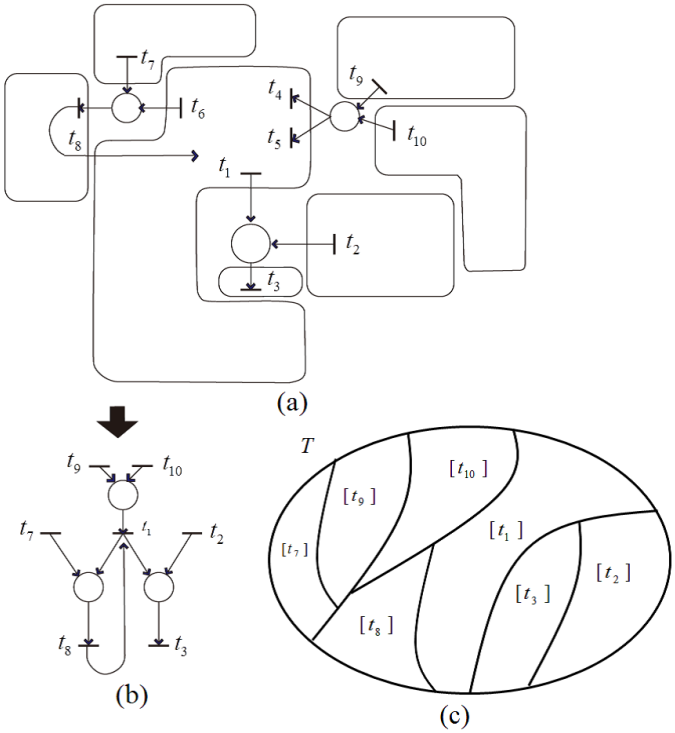

Figure 16. Shrink example of Petri net model and its equivalence classes. (**a**) transitions surrounded by a line satisfies a dependent relation; (**b**) transformed net by applying dependent shrink; (**c**) equivalence classes.

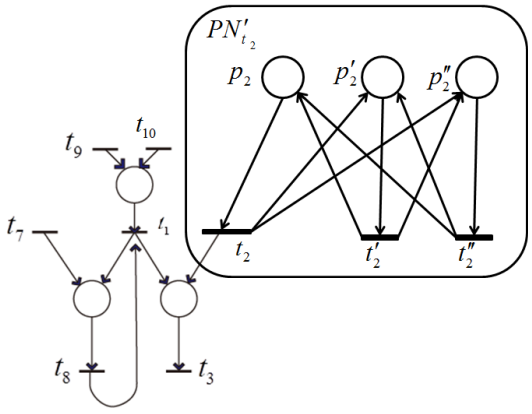

Figure 17. Example structure that cannot be shrunk into a single transition.

6. Conclusions

Despite the recent rapid progress in high throughput measurements of biological data, it is still difficult to gather all reaction speed data in the biological pathways. Particularly for signaling pathways, owing to their complex structure, including protein formations and enzyme reactions, computational methods are essential to estimate as much reaction data as possible from biologically-valid data. In this paper, we presented an algorithm to shrink the transitions in a timed Petri net model into a smaller number of transitions based on their dependency with respect to the firing frequency and, equally, their amount of delay.

We have first introduced a new concept, called the dependency relation, over a set of transitions of a Petri net model representing a signaling pathway, which is in fact an equivalence relation over transitions. Through a structural analysis, we obtained several properties, one important result of which is that shrinking a connected subnet, induced by transitions with a dependency relation, into a transition never affects other parts of a Petri net. Based on these results, we designed an Algorithm 1 with time complexity $O(|P||E|)$ to reduce the Petri net size by applying a dependent shrink process for two elementary structures, i.e., a "single-input and single-output structure" and a "conflict structure", in order to efficiently find a transition set with a dependency relation. A case study was conducted by applying our algorithm to the signaling pathway Petri net model of IL-3, and as a result, IL-3 finally becomes a single transition, which means that all reaction speeds of IL-3 are dependent on one another and that measuring one reaction speed can help in deriving all other speeds.

Our proposed method can be applied not only to signaling pathways, but also to other biological pathways in which retention-freeness holds, for example to metabolic pathways. If, in a timed Petri net model constructed from such a biological pathway, there exists a transition violating retention-freeness, then some discrepancy should happen in the biological pathway, i.e., missing interaction and/or extra interaction, which will be caused by mutations or alternations to the pathway. Such a biological inconsistency is expected to be found with our technique.

We have also pointed out that there may remain some subnets with a dependency relation in the resultant net after applying Algorithm 1 because only a dependent shrink of a "single-input and single-output structure" and a "conflict structure" are adopted. We indicated that this can be resolved by solving a series of linear equations for such a subnet without taking up too much computation time because the size of the subnet should be much smaller compared with the original net. As future work, we are planning to: (1) develop a method to find such a subnet that includes only the places possessing a single-output and multiple-input transitions with a dependency relation; (2) design an algorithm to find the transitions with a dependency relation from the solution of a series of the prior mentioned linear equations; (3) extend our method to a stochastic Petri net by taking into account probabilistic firing delay times.

Supplementary Materials: The following are available online at http://www.mdpi.com/1999-4893/10/1/4/s1, Figure S1: Phenomenon model of the endocytosis signaling pathway, which is obtained from Petri net pathways (http://genome.ib.sci.yamaguchi-u.ac.jp/pnp/), Figure S2: Original endocytosis Petri net model, to which Algorithm 1 is to be applied, Figure S3: An intermediate net is obtained by shrinking all of the self-loops related to transitions, t_2, t_7, t_8, t_{11}, t_{14}, t_{21}, t_{22} and t_{26}, and all of the conflict structures related to transition sets, $\{t_2, t_3\}$, $\{t_7, t_8, t_{11}, t_{14}\}$, $\{t_8, t_{10}\}$, $\{t_{11}, t_{13}\}$, $\{t_{16}, t_{18}\}$, $\{t_{11}, t_{22}, t_{23}\}$, $\{t_{21}, t_{22}\}$, $\{t_{26}, t_{28}\}$ and $\{t_{26}, t_{30}\}$. As a result, t_3, t_7, t_8, t_{10}, t_{13}, t_{14}, t_{18}, t_{21}, t_{22}, t_{23}, t_{28} and t_{30} are shrunk, Figure S4: An intermediate net is obtained by processing single-input single-output structure related to places, Rab5a/GTP, ErbB1, active-SPRY2, Grb2-2, Grb2/c-Cbl, active-SPRY2/c-Cbl, EGFR-2, SHP1 and SHP2, and as a result, t_1, t_5, t_{16}, t_{19}, t_{25}, t_{27} and t_{29} are shrunk, Figure S5: The resultant nets of the final and one step before, XML S1: IL-3, XML S2: endocytosis, PNML S1: IL-3, PNML S2: endocytosis.

Acknowledgments: This work was partially supported by the Grant-in-Aid for Scientific Research (B) (16H02896) from the Japan Society for the Promotion of Science.

Author Contributions: Atsushi Mizuta and Qi-Wei Ge wrote the proofs and designed the algorithm. Qi-Wei Ge and Hiroshi Matsuno conceived of the principle of the Petri net-based modeling of a signaling pathway. Writing of the paper was shared with these three authors. All authors have read and approved the final manuscript.

Conflicts of Interest: The authors declare no conflicts of interest.

References

1. Reisig, W. *Petri Nets: An Introduction*; Springer: Heidelberg, Germany, 1982.
2. Peterson, J.L. *Petri Net Theory and the Modeling of Systems*; Prentice Hall: Englewood Cliffs, NJ, USA, 1981.
3. Wingender, E. (Ed.) *Biological Petri Nets*; IOS Press: Amsterdam, The Netherlands, 2011.
4. Reddy, V.N.; Mavrovouniotis, M.L.; Liebman, M.N. Petri net representation in metabolic pathway. In Proceedings of the First International Conference on Intelligent Systems for Molecular Biology, Bethesda, MD, USA, 6–9 July 1993; pp. 328–336.

5. Schuster, S.; Bandekar, T.; Fell, D.A. Detection of elementary flux modes in biochemical networks: A promising tool for pathway analysis and metabolic engineering. *Trends Biotechnol.* **1999**, *17*, 53–60.
6. Voss, K.; Heiner, M.; Koch, I. Steady state analysis of metabolic pathways using Petri nets. *In Silico Biol.* **2003**, *3*, 367–387.
7. Zevedei-Oancea, I.; Shuster, S. Topological analysis of metabolic networks based on Petri net theory. *In Silico Biol.* **2003**, *3*, 323–345.
8. Heiner, M.; Koch, I. Petri net based model validation in systems biology. In Proceedings of the International Conference on Application and Theory of Petri Nets, Bologna, Italy, 21–26 June 2004; pp. 216–237.
9. Hofestädt, R.; Thelen, S. Quantitative modeling of biochemical networks. *In Silico Biol.* **1998**, *1*, 39–53.
10. Doi, A.; Fujita, S.; Matsuno, H.; Nagasaki, M.; Miyano. S. Constructing biological pathway models with hybrid functional Petri nets. *In Silico Biol.* **2004**, *4*, 271–291.
11. Popova-Zeugmann, L.; Heiner, M.; Koch, I. Time Petri nets for modelling and analysis of biochemical networks. *Fundam. Inform.* **2005**, *67*, 149–162.
12. Lee, D.; Zimmer, R.; Lee, S.; Hanish, D.; Park S. Knowledge representation model for systems-level analysis of signal transduction networks. *Genome Inform.* **2004**, *15*, 234–243.
13. Choi, C.; Crass, T.; Kei, A.; Kel-Margoulis, O.; Krull, M.; Pistor, S.; Potapov, A.; Voss, N.; Wingender, E. Consistent re-modeling of signaling pathways and its implementation in the TRANSPATH database. *Genome Inform.* **2004**, *15*, 244–254.
14. Heiner, M.; Koch, I.; Will, J. Model validation of biological pathways using Petri nets—Demonstrated for apoptosis. *Biosystems* **2004**, *75*, 15–28.
15. Sackmann, A.; Heiner, M.; Koch, I. Application of Petri net based analysis techniques to signal transduction pathways. *BMC Bioinform.* **2006**, *7*, 482.
16. Grafahrend-Belau, E.; Schreiber, F.; Heiner, M.; Sackmann, A.; Junker, B.H.; Grunwald, S.; Speer, A.; Winder, K.; Koch, I. Modularization of biochemical networks based on classification of Petri net t-invariants. *BMC Bioinform.* **2008**, *9*, 90.
17. Heiner, M. Understanding network behavior by structured representations of transition invariants. In *Algorithmic Bioprocess*; Condon, A., Harel, D., Kok, J.N., Salomaa, A., Winfree, E., Eds.; Springer: Heidelberg, Germany, 2009; pp. 367–389.
18. Li, C.; Suzuki, S.; Ge, Q.W.; Nakata, M.; Matsuno, H.; Miyano, S. Structural modeling and analysis of signaling pathway based on Petri nets. *J. Bioinform. Comput. Biol.* **2006**, *4*, 1119–1140.
19. Ruths, D.; Muller, M.; Tseng, J.; Nakhleh, L.; Ram, P.T. The signaling Petri net-based simulator: A non-parametric strategy for characterizing the dynamics of cell-specific signaling networks. *PLoS Comput. Biol.* **2008**, *4*, e1000005.
20. Ruths, D.; Nakhleh, L.; Ram P.T. Rapidly exploring structural and dynamic properties of signaling networks using PathwayOracle. *BMC Syst. Biol.* **2008**, *2*, 76.
21. Lucia, N.; Daniele, M.; Francesca, C.; András, H.; Andrea, P.; Massimiliano, D.P.; Simona, P.; Matteo, S.; Andrea, V.; Federico, B.; et al. On the use of stochastic Petri nets in the analysis of signal transduction pathways for angiogenesis process. In Proceedings of the International Conference on Computational Methods in Systems, Bologna, Italy, 31 August–1 September 2009; pp. 281–295.
22. Li, C.; Ge, Q.W.; Nakata, M.; Matsuno, H.; Miyano, S. Modeling and simulation of signaling transductions in an apoptosis pathway by using timed Petri net. *J. Biosci.* **2007**, *32*, 113–127.
23. Miwa, Y.; Murakami, Y.; Ge, Q.W.; Li, C.; Matsuno, H.; Miyano, S. Delay time determination for the timed Petri net model of a signaling pathway based on its structural information. *IEICE Trans. Fundam.* **2010**, *93*, 2717–2729.
24. Murakami, Y.; Ge, Q.W.; Matsuno, H. Incorporation of cycles and inhibitory arcs into the timed Petri net model of signaling pathway. *IEEE Trans. Fundam.* **2013**, *96*, 514–524.
25. David, R.; Alla, H. *Discrete, Continuous, and Hybrid Petri Nets*; Springer: Heidelberg, Germany, 1998.
26. Onaga, K.; Ge, Q.W.; Ono, N. On optimizing the initial token distribution for a periodic Petri net firing sequence with prescribed firing numbers. *Trans. SICE* **1987**, *23*, 1076–1083.
27. Petri Net Pathways. Available online: http://genome.ib.sci.yamaguchi-u.ac.jp/pnp/(accessed on 28 December 2016).
28. Chen, W.; Daines, M.O.; Khurana Hershey, G.K. Turning off signal transducer and activator of transcription (STAT): The negative regulation of STAT signaling. *J. Allergy Clin. Immunol.* **2004**, *114*, 476–489.

29. Kisseleva, T.; Bhattacharya, S.; Braunstein, J.; Schindler, C.W. Signaling through the JAK/STAT pathway, recent advances and future challenges. *Gene* **2002**, *285*, 1–24.
30. De Groot, R.P.; Coffer, P.J.; Koenderman, L. Regulation of proliferation, differentiation and survival by the IL-3/IL-5/GM-CSF receptor family. *Cell. Signal.* **1998**, *10*, 619–628.
31. System Biology Markup Language. Available online: http://sbml.org (accessed on 28 December 2016).
32. Petri Net Markup Language. Available online: http://www.pnml.org (accessed on 28 December 2016).